

# Searching for Supersymmetry with the $\alpha_T$ variable in $p\bar{p}$ collisions with the CMS Detector at the Large Hadron Collider

*Zoe Hatherell*

A thesis submitted in fulfilment of the requirements  
for the degree of Doctor of Philosophy  
to Imperial College London  
December 2011

# Chapter 1

## Event Reconstruction

The data stored directly from the CMS detector readout contains only the most basic level of information of a collision. As the particles created in the event pass through the detector they create signals at each point they interact, and these signals are locally reconstructed as a series of “hits”. This raw data is stored in CMS as the data format RAW. In order to undertake physics analyses the information is needed in terms of the four-vectors of particles. In order to interpret the raw data in terms of these physics objects a computational process known as object reconstruction is applied to the data. Using knowledge of the behaviour of each type of object and understanding of the detector, the objects are built from the hits, in such a way that optimises the efficiency for each type of object. Varying sets of requirements called “identification” or ID can then be applied to these objects at the analyses level to achieve the level of purity required.

The reconstruction of physics objects happens both within a sub-detector, and also by combining information from two or more sub detectors. The reconstruction is performed under the CMS Software framework (CMSSW) and the reconstructed data is stored in RECO format for use by individual analyses. The main focus of the analysis in this thesis requires well constructed jets and  $\cancel{E}_T$ , while electron, muon and photon objects are also required for vetoes and control samples.

## 1.1 Beamspot

The beamspot represents the locus of the region of beam collision in the detector, where the two bunches of protons meet. It is not an event-by-event measurement, but rather a property of a given physics run, measured over time. It is an important component of reconstruction, as it is used as an estimate of the primary vertex, which is the position a given pair of protons interact to produce an event.

If the beamspot was at the origin of the CMS detector one would expect the distribution of the track closest approach angle  $\phi_0$  to be flat in the transverse impact parameter  $d_{xy}$ . If the beamspot is displaced this behaviour disappears, and thus for each run a fit is made on all available reconstructed tracks to regain this flat behaviour by adjusting the point that  $d_{xy}$  is with respect to, yielding the true beamspot.

## 1.2 Tracks

Whilst not a physics object in its own right, one of the most important elements of object reconstructions involves the identification of tracks left by charged particles in the inner tracker. There can then be used along with other sub detectors when reconstructing charged physics objects. In addition these tracks allow a precision identification of the vertex of interaction. In CMS an algorithm called the Combinatorial Track Finder (CTF) [1] is used to construct tracks from their representative hits.

The reconstruction of a track starts with the construction of a “seed”, an initial candidate track. It contains only a small subset of the available information from the tracker, but must be made up of at least 3 hits, or two hits and an additional beam constraint. The seed represents the initial estimate of the track’s trajectory, from which to collect its additional hits.

In order to achieve the best possible estimate, the seed is built from hits in the innermost area of the tracker, for three important reasons. Although in general the average occupancy decreases with  $r$ , the high-density nature of the pixel detector ensures the inner layer of pixel detectors has an occupancy lower than that of the outermost strip detectors. In addition, the pixel detectors give a better estimate of the trajectory due to their truly 2D measurements, and constructing them in the innermost layer minimises the material budget encountered, as not

all particles will reach the outer layers.

The next element of CTF is a pattern recognition module based on a Kalman Filter [2], that proceeds from the seed outwards and includes any additional hits associated with the basic estimated trajectory. As each new measurement is incorporated to the track the trajectory becomes more accurate. This proceeds for each track candidate in parallel, and where several hits are compatible several new candidates are created.

In order to safeguard against reconstructing one particle as more than one track, an ambiguity resolution mechanism is needed. Given any pair of track-candidates, the fraction of shared hits in the candidate with the fewest hits is examined, and if found to be greater than 50% this track is removed. If the number of hits is identical then that of the lower  $\chi^2$  remains while the other is removed.

Once all compatible hits have been incorporated the most accurate value of the track parameters can be extracted using a final fit. At this point any hits assigned to the track but otherwise not compatible with the track, based on the  $\chi^2$  of the expected residual, are deemed outliers and discarded before refitting. From the tracks selected, many will be fakes, known as “ghost” tracks, removed through a set of criteria based upon quality of fit ( $\chi^2$ ), the transverse and longitudinal impact parameters  $d_0$  and  $d_z$  and the compatibility of the track with what is identified as the interaction vertex.

The fully CTF algorithm is used iteratively, starting with a pool of all hits identified in that event. After one iteration those hits that have been assigned to a track are removed from the pool, successful tracks are stored, and the process continues with the remaining hits. This process has 6 iterations, decided by the type of seed built. The first two are three-pixel seed and two-pixel seeds respectively, and pick up the high  $p_T$  tracks of an event. The second and third are also three and two pixel seeds, but with quality criteria loosened as most of the hits have been taken previously. The fifth and sixth iterations allow a seed to be built from strip detectors to include tracks which are not covered by the pixel volume.

## 1.3 Vertex

The exact location of the initial p-p collision of a given event is not necessarily the same as the beamspot (although this can be used as a reasonable estimate) due to the unknown location of a given proton within the bunch. Known as the “primary interaction vertex”, this is reconstructed using the track collection. Prompt tracks are selected based on quality criteria such as the number of hits in each tracker sub detector, the  $\chi^2$  of the fit and the transverse impact parameter. These are then clustered in  $z$ , and an adaptive vertex fit is used [3], where each track receives a weight between 0 and 1 due to its compatibility to the vertex common to the set of tracks [4].

## 1.4 Jets

The QCD property of confinement makes the treatment of partons in collider physics more complicated, as they hadronise once created and are not identified singularly. Additionally these primary hadrons can both emit gluons and decay and fragment into lighter hadrons. These decay products are all travelling in the same direction, as they have been “boosted” by the momentum of the primary hadron, so each of these groups of particles is called a “jet”. Physics analyses then make requirements on these jets, as opposed to specific requirement of quarks and gluons, where the “jet” concept in a perfect detector should represent the four-vector of the primary hadron. This is achieved through jet reconstruction where all information left in the detector from the decay products are assigned and added to a jet. As the products are moving under the same boost the jet can be thought to have a cone shape extending from the interaction vertex, where the radius of the cone is defined in the  $\eta - \phi$  plane,  $R = \sqrt{\Delta\eta^2 + \Delta\phi^2}$

At a hadron collider such as the LHC hadronic processes are abundant, and thus the method of defining and reconstructing these jets is crucial to and physics analyses. In CMS there are types of reconstructed jets available, based on the sub-detectors used: Calorimeter Jets (CaloJets) use only the ECAL and HCAL, Jet Plus Tracks (JPT) Jets include also information from the tracker, and Particle Flow (PF) Jets use information from the whole detector whilst reconstructing all particles in parallel. The analysis in this thesis uses CaloJets, the reconstruction of which is discussed in more detail below.

The purpose of jet reconstruction is to group a set of boosted particles together, achieved by an algorithm that "clusters" the information from the calorimeters. The energy deposited in ECAL and HCAL cells are first combined into what are known as "calorimeter towers", consisting of one or more HCAL cells combined with the ECAL cells which geographically align to the HCAL cell. The tower energy is defined by the sum of cell energies passing an energy threshold to protect against electronic noise. Towers that fulfil the requirement of  $E_T > 0.3\text{GeV}$  then form the input to the clustering algorithm used by CMS, anti- $k_T$  [5].

### 1.4.1 The anti- $k_T$ jet clustering method

Due to the expected levels of hadronic activity at the LHC, the jet clustering algorithm must be fast. In addition, it must be stable against the addition of soft particles, called "infra-red safe", as partons may emit soft gluons. It must also be "collinear safe", meaning it yields the same jets if a parton were to split into two collinear partons, so that they would both end up in the same jet. These two conditions are essential so that the experimental data may be compared to theoretical calculations regardless of the order they are performed at.

The anti- $k_T$  clustering method [6] is a sequential recombination algorithm that fulfils these criteria [7], working pair-wise to combine nearby towers starting with those highest in  $p_T$  first. The decision of which order to combine pairs in is achieved with the use of two distance metrics, the distance  $d_{ij}$  between two towers  $i$  and  $j$ , and the distance  $d_{iB}$  between the  $i$ th tower and the beam. Considering all possible combinations of both metrics, the smallest is identified.

If this smallest value is the first case, the two towers  $i$  and  $j$  are combined into one prototype jet, whose position is weighted by the momenta of its parts. If it is the second case, the tower  $i$  is identified as a jet and removed from the list. This process is continued with the updated towers and prototype jets, until all towers have been combined. The definition of the metrics are seen in Equations 1.1 and 1.2 where  $\Delta_{ij}^2 = (y_i - y_j)^2 + (\phi_i - \phi_j)^2$ .

$$d_{ij} = \min(k_{ti}^{2p}, k_{tj}^{2p}) \frac{\Delta_{ij}^2}{R^2} \quad (1.1)$$

$$d_{iB} = k_{ti}^{2p} \quad (1.2)$$

Tower  $i$  has transverse momentum  $k_{ti}$ , rapidity  $y_i$  and azimuth  $\phi_i$ . The variable  $R$  is analogous to the cone radius definition described above, and for this analysis  $R = 0.5$ . This general form of the metrics governs several types of jet algorithm of this family, differing in the value of power  $p$ . This is the parameter responsible for the relative importance of momenta and distance, and for anti- $k_T$   $p = -1$  placing the importance on the momenta, and giving the “anti” in its name (after another variant, the  $k_T$  algorithm for which  $p = +1$  [8]).

In this algorithm a hard particle creating a large energy deposit with no other hard deposits surrounding it will gather in the soft particle deposits. If another hard particle is found within  $2R$  then the soft deposits are shared between them with weights relative to the hard particle momenta, unless they are within  $R$  of one another in which case they are identified as one jet.

The shape of the jet is defined alone by the cone about the hard particle, resulting in a perfectly conical jet except in the case where more than one hard particle exists within  $2R$ . If the two hard jets are within  $R$  of one another, the shape is either dominated by the hardest if there is a significant difference in the momenta, or if they are similar, defined by the total area covered by both cones. If the jets are not within  $R$  but within  $2R$ , there is not space for each jet to be conical, so either the hardest jet is conical and the softer is missing a piece, or if they have similar momenta each has a chunk missing with a boundary line down the middle of the shared area. Figure 1.1 shows in the  $y$ - $\phi$  plane jets reconstructed by anti- $k_T$  for a sample event (generated by Herwig [9]) in which many soft deposits exist. Many coloured circular jet patterns are seen, representing conical jets, as well as the cases with close hard deposits demonstrating the shared and clipped jet area shapes.

Contamination from both pileup and underlying events can contribute soft energy deposits which may affect the momenta of jets reconstructed, the effect of which is known as the “back reaction”. One of the major advantages of the anti- $k_T$  algorithm is that due to the relative importance of hard deposits over softer deposits this effect is suppressed, allowing more accurate measurement of jet momenta than other comparable models, leading to its selection by CMS.

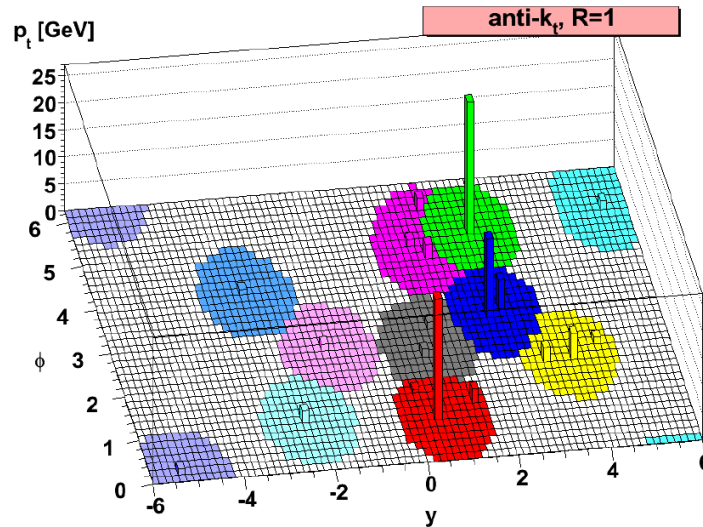


Figure 1.1: Illustration of the reconstructed jets for a sample Herwig generated event, with many soft deposits. Each coloured area represents the shape of the jet reconstructed, illustrating the trend to a conical nature of anti- $k_T$ , and the behaviour of the algorithm where two hard deposits are close. Taken from [6].

### 1.4.2 Jet Energy Scale Corrections

The jets reconstructed in the detector using the method above typically have an energy that is different to that we would measure in a perfect situation. This is due to the nature of the response of the calorimeters, which is non-linear and non-uniform, as well as any residual effect contributed from pileup and underlying events (although this is small as mentioned above). For this reason, reconstructed jets must undergo energy corrections before they can be used in physics analyses.

The aim of these Jet Energy Scale (JES) corrections is to relate the energy measured in the detector to the energy of the underlying jet particles through knowledge of the detector response. There are three typical levels of correction

**L1 - Offset** An offset is subtracted to remove the energy contributions that are not associated with the event but rather from electronic noise and pileup events.

**L2 - Relative** Next the value is multiplied by a factor which is a function of a given pseudorapidity  $\eta$  to correct the relative differences in responses in different regions of the calorimeters.



**L3 - Absolute** Finally the value is multiplied by a second factor, which corrects the variable response to different jet  $p_T$ . The response to a given particle never returns the entire proportion of energy, and the percentage returned depends heavily on the momenta of the particle.

For the current dataset presented in this thesis, only L2 and L3 corrections were applied (L2L3), as L1 corrections deemed unnecessary due to low expected pileup rates at low luminosity. The combined L2L3 correction is performed using a combination of Monte Carlo calibration and corrections using data-driven methods. However crosschecks were made with the L1 offset included to ascertain validity of this assumption.

Initially an estimate of the correction is calculated with the help of Monte Carlo truth information, representing the major portion of the calibration. Here instead of separating the three levels, an all-together approach is used where relative and absolute are tackled simultaneously. Events generated by PYTHIA [10] are passed through the full CMS detector simulation GEANT 4 [11], in order to identify the reconstructed jets. In addition, full information for the real physical jet, known as a *generator* jet is retained. Each reconstructed jet is matched its own generator jet in the  $\eta - \phi$  plane, making a requirement on the cone radius  $R \leq 0.25$  to avoid mis-matching. A comparison of the momenta of the reconstructed jet and the generator jet allows a calibration factor to be extracted relative to the jet's  $\eta$  and  $\phi$ .

Having calibrated the momenta using Monte-Carlo data-driven corrections of the relative and absolute calibrations are made. The relative correction is extracted using di-jet events balanced in  $p_T$  where one is detected in the central region, and the other may have any  $\eta$  value. The measurement of the second jet energy is compared to the well-defined measurement of the central region (chosen as the control region as it delivers the best performance for high  $p_T$  jets) in order to return the correction factor dependant on  $\eta$ . Having applied this correction, another is performed for the absolute using an events where a photon lies back to back with a jet. Comparing the momenta of the two gives an understanding of the distribution of the percentage of energy that has been included in a jet yielding the required factor.

With the application of the steps of calibration, the total energy of the particles within the jet has been recovered to an acceptable level required by

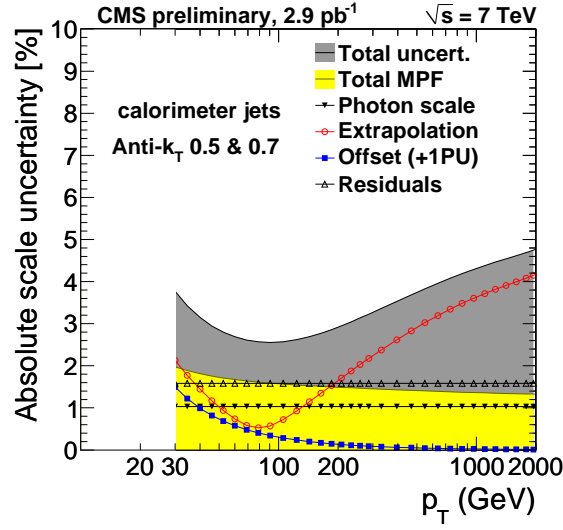


Figure 1.2: Total uncertainty (grey) of jet energy scale with respect to  $p_T$  after full L1L2L3 corrections applied for  $2.9\text{pb}^{-1}$  of 7TeV data at CMS. Individual uncertainties of algorithm components shown also. Taken from [12].

the physics analyses of CMS. The full L1L2L3 corrections have a precision corresponding to an 3 – 6 % uncertainty of the jet energy scale (JES) for jet momenta ranging from 30 GeV up to 2TeV, as illustrated in first 7TeV collisions in Figure 1.2 [12].

## 1.5 Missing Energy

Alongside reconstruction of physics objects comes the calculation of “missing energy”, an important signal. In the Standard Model, neutrinos pass through the detector without interacting and therefore are responsible for energy “gone missing”, alone of the known particles. However in some New Physics models, most notably SUSY, there are suggestions of other more massive particles that would exhibit this signature.

As previously mentioned the LSP if it exists would not react, meaning its typical signature in a detector is that of energy gone undetected. This is observed as a momentum imbalance, or “missing energy” of the observed particles. In an ideally hermetic detector this would be a simple measurement through a vectorial sum of all existing energy deposits. However, even the best detector design cannot avoid the requirement of an opening through which the beams enter the detector,

and thus any particles moving toward this forward region may escape detection, thus spoiling the accuracy of the missing energy constraint.

Although these particles may have considerable momenta in the direction of the beam axis, in order to have an  $\eta$  outside the range of the calorimeters  $-5 < \eta < 5$  its momentum transverse to the beam  $p_T$  must be less than  $0.013E$  where  $E$  is its total energy. This ensures the transverse momentum lost to particles outside the acceptance is very small, thus an imbalance can indicate a particle leaving no deposit. The imbalance is referred to as *missing transverse energy*,  $\cancel{E}_T$ , the magnitude of the 2D vector of missing  $p_T$ , which is written as  $\vec{\cancel{E}}_T$ . The reconstruction of these in CMS can occur in several ways, but the construction of calorimeter  $\cancel{E}_T$  (caloMET) involves the summation of all  $n$  calorimeter towers in an event given in Equations 1.3 and 1.4 [13].

$$\vec{\cancel{E}}_T = - \sum_n E_n (\sin\theta_n \cos\phi_n \hat{\mathbf{i}} + \sin\theta_n \sin\phi_n \hat{\mathbf{j}}) \quad (1.3)$$

$$\cancel{E}_T = |\vec{\cancel{E}}_T| \quad (1.4)$$

### 1.5.1 $\cancel{E}_T$ Corrections

The energy deposits from the calorimeter towers summed are the uncorrected values, which like before in the jet reconstruction also require corrections, separated into two types. Type I corrections take into account the JES corrections described earlier in Section 1.4.2, as well as corrections to take care of muons and hadronic taus in an event. Type II accounts for effects from pile-up or underlying soft events.

#### Type I Corrections

The Type I corrections account for corrections associated with physics object measurements. Firstly, as the JES corrections for jets are relevant to the  $\cancel{E}_T$  reconstruction also, a correction must be applied to bring  $\cancel{E}_T$  in line with the true energy of the jets. The relevant correction described in Section 1.4.2 to each jet that has a corrected  $p_T \geq 20\text{GeV}$  and an Electromagnetic Fraction (EMF)  $\leq 0.9$  is used to modify  $\vec{\cancel{E}}_T$ . The requirement on the EMF prevents applying the corrections in the case of an electron reconstructed as a jet, as this will have a

high fraction of electromagnetic energy.

The  $\cancel{E}_T$  measured in the calorimeters must be then corrected for any muon present, as a muon would pass through the calorimeter volume without depositing much of its energy. The information regarding a muon in the event is measured and reconstructed accurately using both the tracker and the muon system (see below). Having added any deposits the muon has made to the calorimeter to the  $\vec{\cancel{E}}_T$  the  $p_T$  of the muon can then be subtracted to remove the effect of the missed muon on the  $\cancel{E}_T$ . This is done for each reconstructed muon that is reconstructed using both Muon algorithms (see Section 1.6) and passes a set of quality criteria. Among these cuts is a requirement on the isolation of the muon, as not all deposits in a non-isolated muon would be from the muon itself, and therefore would result in an over correction [14].

An additional correction is needed to account for the case of a tau that decays hadronically, as these tau-jets have differing characteristics from other jets. They are likely to have a low particle multiplicity where each product carries a significant energy, as opposed to the usual case of high-multiplicity soft products. In the region used for jet reconstruction  $R \lesssim 0.5$  about the tau,  $\vec{\cancel{E}}_T$  is summed, and the true energy of the tau removed from it in order to yield the correction necessary.

## Type II Corrections

Having corrected all the hard jets this second step of corrections addresses the jets outside the type I acceptance and any energy deposits not clustered into jets, to remove the effects of underlying events and pile-up. This is obtained using a Monte Carlo control samples of events with a Z decay to two electrons, as characteristically the Z has low  $p_T$  and there is much unclustered energy. The sum of momenta of the towers unclustered into jets  $\vec{U}$  is obtained by taking the uncorrected  $E_T$  of an event, removing the momenta of the uncorrected jets and of the electrons.  $\vec{U}$  is then corrected using the Monte Carlo truth information [15].

### 1.5.2 Using Jets for Missing Energy - $\cancel{H}_T$

Another type of  $\cancel{E}_T$  reconstruction is possible, when the hadronic missing energy is created using the vectorial sum of the reconstructed jets of an event. This type is known as  $\cancel{H}_T$ , defined in Equation 1.5 where  $p_T^n$  is the transverse momentum

of the  $n$ th jet. In a hadronic event with no other standard physics objects other than jets is analogous to a  $\cancel{E}_T$  measurement, albeit relying only on the jet reconstruction.

$$\cancel{H}_T = | - \sum_n p_T^n | \quad (1.5)$$

The advantage of using  $\cancel{H}_T$  is that unclustered energy is automatically not a part of the sum, so automatically this variable is less sensitive to detector effects and pile-up than  $\cancel{E}_T$ , and therefore more robust, making it desirable for early measurements at the LHC. However through the same logic, it may fail to include real jets that are below the threshold, or unclustered energy that did belong to the event, factors which affect its resolution.

## 1.6 Muon

Muons are reconstructed in CMS by combining the information recorded in the muon systems with reconstructed tracks from the tracker. The small number of deposits made by muons in the calorimeter systems are not used in reconstruction although are used in muon identification criteria. The reconstruction of tracker tracks have been described already in Section 1.2.

In the muon chambers a local reconstruction occurs also, creating a *standalone muon track* [16]. Seeds are generated from track segments created by fitting adjacent hits within the layers of the DT or CSC detectors. As in the tracker, the seed suggests an initial estimate of the muon four-vector, and the fit is then extended to include segments from all the sub detector types, again using a Kalman Filter. Duplicates known as ghosts exist where one muon gives rise to more than one seed, thus tracks that share hits are compared and the best kept. Tracks are then constrained by the beam spot position within uncertainty in order to improve momentum measurement.

Once local reconstruction in the tracker and muon chambers is complete, they are passed to global muon reconstruction. There are two algorithms of muon reconstruction which are both used in parallel to create two type of candidate muons, depending on the direction of the extrapolation between tracker and muon systems.

**Global Muons** These muons are reconstructed from the “outside - in”. Starting

with a standalone muon, a match is made back to a reconstructed track before a fit is made to the combination. This works especially well for muons that carry high  $p_T$ , greater than 200 GeV, as within this limit the muon systems have greater resolution and thus are superior to the tracker information.

**Tracker Muons** These muons reconstructed from the “inside-out”. Here, all tracks of  $p_T > 0.5$  GeV are treated as if they possibly came from muons. Each of these muon candidates is followed through to the muon system, allowing for possible energy losses and scattering. If any muon segment track is identified as a match, then the resulting track is considered a muon. As this only requires one single segment in the muon system this reconstruction method is most accurate for low momentum muons where the full volume of the muon system is not reached.

Providing they carry significant momentum muons in CMS collisions are mainly reconstructed as one of these types, and may often be reconstructed as both. However, about 1% of muons produce a standalone muon track only, and no matching tracker track is found. These are also retained.

The muon collection contains candidates from all three cases. Where the same track from the tracker has been involved in the reconstruction of both a Global and a Tracker muon, they are merged into one. The standalone muon tracks only included in the case where no other reconstruction used any of the muon segments. Combining the algorithms gives the best efficiency for the muon collection, and requirements of which to allow for analysis can be set later in Muon Identification criteria [17].

## 1.7 Photons

Photons are reconstructed solely with the information from the energy deposited in the ECAL. As a photon traverses the tracker material prior to the calorimeter system, photon conversions can occur. In addition, a primary electron travelling in the detector also loses energy through bremsstrahlung and corresponding photons are emitted tangentially to its curved trajectory. This leads to a characteristic energy pattern spread out in  $\phi$  as the trail of photons is left but

narrow in  $\eta$  under the strong magnetic field. A clustering algorithm is therefore used to gather the energy from one primary particle into a SuperCluster (SC).

Different algorithms are required depending on the geometry - the “Hybrid” algorithm is used in the barrel, and the “Multi5x5” in the end-caps [18]. The Hybrid algorithm selects “dominoes”, strip-like collections of crystals in this  $\eta - \phi$  geometry, whereas in the end-caps the structure is not arranged in  $\eta - \phi$  and therefore Multi5x5 clusters each seed in a 5x5 crystal window, and allows combination with other overlapping 5x5 clusters.

Energy corrections must be applied to the SC to allow for detector effects in the calorimeter, typically at the 1% level. The weighted average of deposits in the SC determine the candidate location and the relationship between this and the primary vertex gives the direction. From the corrected SC’s photons are reconstructed providing the SC energy corresponds to energy in the HCAL of no more than 15% SC energy, and no matching track is found.

## 1.8 Electrons

The reconstruction of electrons in CMS combines the information from the energy deposits in the ECAL and the information from the tracker. This can be done both beginning with the ECAL and extrapolating to the tracker (ECAL-seeded) or vice versa (tracker-seeded). As the majority of isolated electrons can be reconstructed using the ECAL-seeded approach this is used for the veto in this analysis.

The reconstruction process begins by gathering compatible hits in the ECAL and combining them into a SuperCluster, the same described under Photon reconstruction. The algorithm responsible for generating electron superclusters takes advantage of this, combining individual hits into clusters, and then combining clusters within a narrow path in  $\phi$ .

The tracker tracks left by electrons cannot be merely reconstructed using the method described above, as the high percentage of energy loss due to Bremsstrahlung makes the use of a Kalman Filter unsuitable, as the energy loss is non-Gaussian. Instead, a variant known as the Gaussian Sum Filter (GSF) [19] is more suitable, although slower. A supercluster is matched to a seed in the inner tracker, and the electron track reconstructed by extrapolation and fitted

with the GSF. As the GSF takes more processing power than the Kalman filter a pre-selection is applied to reduce the time taken, based on the compatibility of the track and supercluster in the  $\eta - \phi$  plane [20].



# Bibliography

- [1] Wolfgang Adam, Boris Mangano, Thomas Speer & Teddy Todorov. “Track Reconstruction in the CMS tracker”. Technical Report CMS-NOTE-2006-041, CERN, Geneva (2006).
- [2] R Frhwirth. “Application of Kalman filtering to track and vertex fitting”. *Nucl. Instrum. Methods Phys. Res., A*, **262**, HEPHY-PUB-503 (1987) 444. 19 p.
- [3] R Frhwirth, Wolfgang Waltenberger & Pascal Vanlaer. “Adaptive Vertex Fitting”. Technical Report CMS-NOTE-2007-008, CERN, Geneva (2007).
- [4] The CMS Collaboration. “Tracking and Primary Vertex Results in First 7 TeV Collisions”. **CMS-PAS-TRK-10-005**.
- [5] Xavier Janssen for the CMS Collaboration. “Underlying event and jet reconstruction in CMS”. **CMS CR-2011/012**.
- [6] Matteo Cacciari, Gavin Salam & Gregory Soyez. “The anti- $k_t$  jet clustering algorithm”. *JHEP*, **0804** (2008) 063.
- [7] V Chetluru, F Pandolfi, P Schieferdecker & M Zelinski. “Jet Reconstruction Performance at CMS”. **CMS AN-2009/067**.
- [8] S. Catani, Yuri L. Dokshitzer, M. H. Seymour & B. R. Webber. “Longitudinally invariant  $K(t)$  clustering algorithms for hadron hadron collisions”. *Nucl. Phys.*, **B406** (1993) 187–224.
- [9] G. Corcella, I.G. Knowles, G. Marchesini, S. Moretti, K. Odagiri et al. “HERWIG 6.5 release note”. hep-ph/0210213.
- [10] Torbjorn Sjostrand, Stephen Mrenna & Peter Z. Skands. “PYTHIA 6.4 Physics and Manual”. *JHEP*, **0605** (2006) 026, hep-ph/0603175.
- [11] The Geant4 Collaboration. “Geant4-A Simulation Toolkit”. *Nuclear Instruments and Methods in Physics Research A*, **506** (2003) 250–303.
- [12] The CMS Collaboration. “Jet Energy Corrections determination at 7 TeV”. **CMS-PAS-JME-10-010**.
- [13] S Esen, G Landsberg, M Titov, A DeRoeck, M Spiropolu, M Tytgat, D Puigh, P Wittich, K Terashi, A Gurrola, T Kamon, C. N. Nguyen, A Safonov, J. W. Gary,

- F Liu, H Nguyen, J Sturdy, R Cavanaugh, R Remington, M Schmitt, B Scurlock, E.A. Albayrak, T Yetkin & M Zielinski. “ $\cancel{E}_T$  Performance in CMS”. **CMS AN-2007/041**.
- [14] Greg Landsberg & Filip Moortgat. “MET Reconstruction, Performance, and Validation”. **CMS AN-2008/089**.
- [15] The CMS Collaboration. “Missing Transverse Energy Performance in Minimum-Bias and Jet Events from Proton-Proton Collisions at  $\sqrt{s} = 7$  TeV”. **CMS-PAS-JME-10-004**.
- [16] The CMS Collaboration. “Performance of CMS Muon Reconstruction in Cosmic-Ray Events”. *J. Instrum.*, **5**, arXiv:0911.4994. CMS-CFT-09-014 (2009) T03022 . 47 p.
- [17] The CMS Collaboration. “Performance of muon identification in pp collisions at  $\sqrt{s} = 7$  TeV”. **CMS-PAS-MUO-10-002**.
- [18] The CMS Collaboration. “Photon reconstruction and identification at  $\sqrt{s} = 7$  TeV”. **CMS-PAS-EGM-10-005**.
- [19] Wolfgang Adam, R Frhwirth, Are Strandlie & T Todor. “Reconstruction of Electrons with the Gaussian-Sum Filter in the CMS Tracker at the LHC”. Technical Report CMS-NOTE-2005-001, CERN, Geneva (2005).
- [20] The CMS Collaboration. “Electron reconstruction and identification at  $\sqrt{s} = 7$  TeV”. **CMS-PAS-EGM-10-004**.